

1

Phosphorus Ligand Effects in Homogeneous Catalysis and Rational Catalyst Design

Jason A. Gillespie¹, Erik Zuidema², Piet W. N. M. van Leeuwen³, and Paul C. J. Kamer¹

¹*EaStCHEM, School of Chemistry, University of St Andrews, St Andrews, United Kingdom*

²*SABIC Technology & Innovation, Geleen, The Netherlands*

³*Institute of Chemical Research of Catalonia (ICIQ), Tarragona, Spain*

1.1 Introduction

Over the last 60 years, the increasing knowledge of transition metal chemistry has resulted in an enormous advance of homogeneous catalysis as an essential tool in both academic and industrial fields. The continuously growing importance of transition metal catalysis is well illustrated by the recent awards of three Nobel Prizes in 2001, 2005 and 2010 to this field of chemistry. Remarkably, phosphorus(III) donor ligands have played an important role in several of the acknowledged catalytic reactions [1–5]. The positive effects of phosphine ligands in transition metal homogeneous catalysis have contributed largely to the evolution of the field into an indispensable tool in organic synthesis and the industrial production of chemicals.

An astounding diversity of ligand types and structures is known in literature: mono-, bi- and polydentates, ligands based on single donor atoms (such as phosphorus or nitrogen) or multiple donor atoms (such as P–N or P–O), achiral or chiral ligands, and ligands with exotic steric or electronic constraints. This extensive ligand library is in part the result of the fast developments in organometallic chemistry leading to a wide variety of ligand structures which have been exploited in transition metal complexes. Furthermore, the urge to optimise transition metal complex properties such as catalytic performance triggered an evolutionary type of growth of ligand libraries. Systematic variation and combination of successful ligand structures, intended to optimise ligand performance, inevitably led to new and unprecedented properties, in addition to the expected optimised catalytic systems.

Figure 1.1 represents an extremely tiny sampling of phosphorus donor ligands successful in diverse catalytic reactions, displaying an incredibly large variety in their structure. A striking feature is that ligands of

2 Phosphorus(III) Ligands in Homogeneous Catalysis

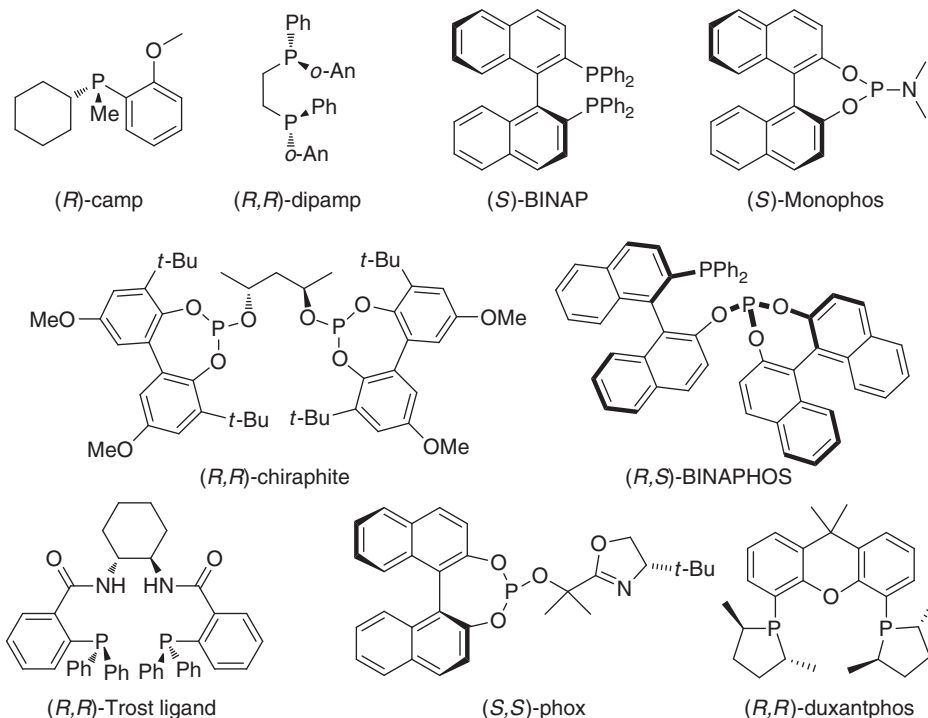


Figure 1.1 Selection of phosphorus(III) ligands.

very different structures can provide similarly high efficiency in the same catalytic reaction while ligands with very similar structures can behave very differently. The first row in Figure 1.1 shows successful ligands in asymmetric hydrogenation. The monodentate ligand *R*-camp provided good enantioselectivity in the asymmetric hydrogenation of dehydro amino acids [6], but Knowles *et al.* showed that bidentate ligands like dipamp performed superior compared to monodentates [7]. Unexpectedly, Feringa and de Vries showed two decades later that monodentates like *S*-monophos can outperform bidentate ligands [8]. The ligands on the second row are structurally quite different and showed different coordination modes in hydridorhodium carbonyl complexes; *R,R*-chiraphite coordinates in bisequatorial fashion in the trigonal bipyramidal rhodium complex [9], whereas binaphos occupies an apical and an equatorial site [10]. Nevertheless, both ligands perform well in asymmetric hydroformylation of styrene. All three ligands of the third row perform well in palladium-catalyzed asymmetric allylic substitution, although the ligands are based on different types of chirality and/or donor atom type [11–13]. Finally, ligands such as BINAP (2,2'-bis(diphenylphosphino)-1,1'-binaphthyl) show excellent performance in several catalytic reactions [1], which instigated Jacobsen to coin such ligands 'privileged' ligands [14].

When designing a new catalyst, the choice of the metal is naturally of utmost importance. This choice is usually dictated by the envisaged catalytic reaction and based on pre-existing knowledge or by screening via trial and error. Although most transition metals are capable of facilitating all elementary steps which constitute a catalytic cycle, several catalytic reactions are dominated by specific metals such as palladium for allylic substitutions and rhodium for the hydroformylation of alkenes. The next step is, in general, adjusting the reactivity of the metal by adding donor ligands. It is not surprising that the nature of the donor atom is pivotal in influencing the reactivity of the metal. The σ -donor and π -acceptor properties as well as the steric congestion imposed on the metal strongly influence the catalyst performance. In the case of bidentate ligands, the

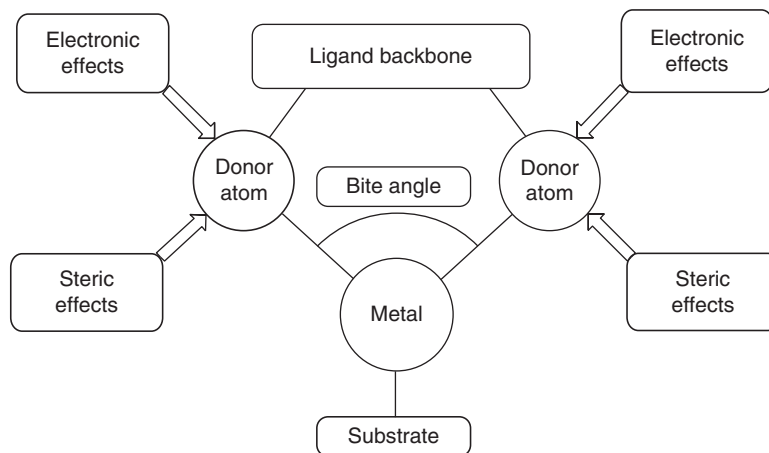


Figure 1.2 Schematic representation of parameters used to design new and optimize existing catalysts.

bite angle enforced on the metal also has a profound effect on the steric and electronic properties of the metal (Figure 1.2). Ligand effects are very powerful, and in fact different combinations of transition metals and donor ligands can result in very similar reactivity. Figure 1.2 shows which points of variation may be considered when designing new bidentate catalysts.

Phosphorus has often been the donor atom of choice, and it has a long history as a soft, strongly ligating atom for late-transition metals, which is easily rationalised by hard/soft acid base theory. Moreover, in-depth understanding of the effects of phosphorus ligands on the properties of transition metal complexes is greatly advanced by facile analysis by ^{31}P NMR spectroscopy; in fact, the many successes of phosphorus ligands in the field of homogeneous catalysis might very well be mainly due to this easy structural (in situ) analysis by NMR.

One of the first examples of the crucial effect of phosphine ligands on catalyst performance was reported in the ‘Reppé’ chemistry, to form acrylic esters from alkynes, alcohols and carbon monoxide [15]. A homogeneous triphenylphosphine nickel iodide complex was the catalyst responsible for the production of acrylic acid from acetylene, carbon monoxide and water. In the same period, another important discovery in the field of homogeneous catalysis was made by Otto Roelen, who accidentally discovered that cobalt carbonyl complexes could convert alkenes into valuable aldehydes by applying high pressures of CO and H_2 [16]. Although commercialisation of these processes was accomplished years later, these discoveries revealed the potential power of homogeneous catalysis and initiated the development of a prosperous field of research in both academia and industry.

The nickel-catalysed hydrocyanation of butadiene as developed and applied by Du Pont is an excellent example of an industrial application in which ligand parameters proved to be crucial [17]. The catalytic reaction employs a nickel catalyst modified by aryl phosphite ligands for the atom economic synthesis of adiponitrile from butadiene and hydrogen cyanide. This seminal application of transition metal catalysis clearly illustrates the level of sophistication which can be achieved in fine tuning the activity and selectivity of the metal centre. Key to the development of this process was a systematic study of ‘ligand effects’ by Tolman which led to the first systematic description of ligand properties in the field of homogeneous catalysis using organometallic complexes [18].

The Tolman steric and electronic parameters proved powerful tools for quantitative and qualitative understanding of the influence of first coordination sphere ligands on transition metal complex properties. The effects of these ligand parameters upon metal–ligand and ligand–substrate interactions are the basis for a rational design approach in catalyst development. The quantification of the steric and electronic contributions of phosphorus(III) ligands to M–P bonding and reactivity has contributed to a large extent to the discovery and improvement of catalytic activity of new phosphine transition metal complexes.

An important boost in the application of phosphorus donor ligands in homogeneous catalysis was triggered by the discovery of $\text{RhCl}(\text{PPh}_3)_3$ as a catalyst for alkene hydrogenation by Wilkinson and co-workers in the mid-1960s [19]. It is fair to say that the mechanism of this reaction is now among the best studied in catalysis research. Studies of electronic and steric ligand effects led to detailed understanding of the elementary reaction steps of the catalytic cycle. Increasing the donor capacity of the phosphine ligands by introducing donating substituents at the aromatic rings attached to the phosphorus atom resulted in higher reaction rates [20]. This work was soon followed by the initial work of Vaska, who showed that oxidative addition of hydrogen to Rh and Ir is one of the important elementary steps of the catalytic cycle [21].

Soon thereafter, phosphorus donor ligands proved to be very effective in rhodium-catalyzed hydroformylation as well. Wilkinson *et al.* showed that rhodium carbonyl complexes modified by alkylphosphines and arylphosphines were active catalysts for the hydroformylation of alkenes under mild conditions (70°C and 100 bar) [22]. Workers at Union Carbide Corporation found that phosphites were also very effective ligands for this reaction and that the catalyst performance was strongly dependent on the type of phosphite [23].

Bidentate ligands lead to increased stability of organometallic complexes due to the chelate effect, which has strong impact on the chemistry at the metal centre. The synthesis of the archetypical diphosphine dppe was already reported in 1959 [24], and Chatt and Hieber [25] explored the coordination chemistry of several diphosphines with an ethane bridge. Slaugh explored the use of dppe in cobalt-catalysed hydroformylation [26], but it did not result in significant changes in catalyst performance compared to the phosphine-free cobalt carbonyl catalyst. The use of alkylphosphines led to the first ligand-modified (cobalt) hydroformylation catalyst (the Shell HydroFormylation process, or SHF). A strong beneficial effect of bidentate ligands was discovered by Keim and coworkers at Shell Development in the late 1960s [27]. Certain bidentates containing an oxygen and a phosphorus donor atom formed excellent nickel catalysts for the oligomerization of ethene. Most efficient ligands were diphenylphosphinoacetic acid or 2-diphenylphosphinobenzoic acid, which was named SHOP ligand after the resulting Shell Higher Olefins Process that came on stream in 1977 (Figure 1.3).

In 1966 Iwamoto and Yuguchi described the first *advantageous* results for a range of diphosphine ligands with varying bridge lengths in the co-dimerisation of butadiene and ethene using iron catalysts [28]. In many other cases, the activity of catalysts containing dppe instead of PPh_3 was lowered due to the strong chelating power of the diphosphine. This anticipated higher stability of chelating diphosphine complexes was seen as a drawback in the development of more active catalysts.

Theoretical work of Thorn and Hoffmann [29] corroborated that migration reactions were slow in complexes containing chelating ligands such as dppe. During the migration process, the neighbouring phosphine ligand was shown to have a tendency to enlarge the P–M–P bite angle, which is prevented by the constrained C_2 bridge of the ligand.

Asymmetric hydrogenation is arguably one of the most mature fields showing beneficial use of bidentate phosphine ligands. In 1971 Kagan reported the use of DIOP for the rhodium diphosphine-catalysed hydrogenation of N-acetylphenylalanine [30,31]. This first indication of improved performance of bidentate ligands compared to monodentates was soon followed by the report of Knowles *et al.* that the P-chiral diphosphine DIPAMP led to excellent enantioselectivities compared to the monodentates CAMP and PAMP [6,7]. This discovery led to the first industrial applications of bidentate phosphines in the production of L-DOPA via the rhodium-catalysed asymmetric hydrogenation by Monsanto. Selke developed the sugar-based bisphosphonite Phenyl- β -GLUP for the same process (Figure 1.4) [32], which has been applied for many years by the German company VEB-Isis. Ever since, many other chiral diphosphines have shown wide applicability in the area of asymmetric hydrogenation, and several applications have been developed. Important new ligands that have been introduced comprise (Figures 1.1 and 1.4) Noyori's BINAP [33], DuPhos (Burk) [34], Takaya's BINAPHOS [10] and C_1 -symmetric ferrocene-based ligands ('Josiphos') introduced by Togni [35].

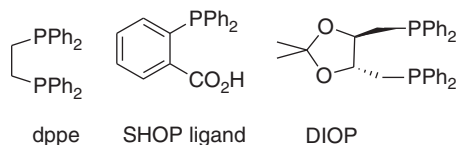


Figure 1.3 Structures of early bidentate phosphine ligands dppe, SHOP ligand and DIOP.

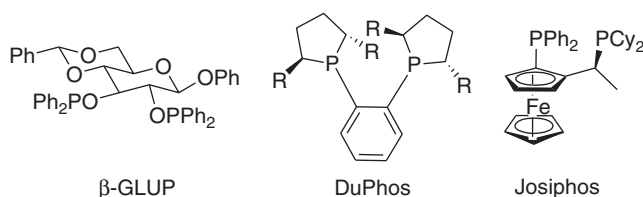


Figure 1.4 Structures of Phenyl- β -GLUP, DuPhos and Josiphos.

Late-transition-metal-catalysed coupling reactions, such as palladium- or nickel-catalysed C–C, C–O and C–N bond formation, have proven to be very sensitive to ligand effects [36]. The amount of data available on ligand effects for these reactions is extensive, although rationalization of trends often remains a challenging task [37].

The efficacy of the Trost ligand in asymmetric allylic alkylation was originally explained by the ‘embracing’ effect of the bidentate ligand [38]. By simply reasoning that larger bite angles would lead to more efficient catalysts, the wide bite angle ligand Duxantphos (Figure 1.1) was successfully designed and applied [13]. Detailed mechanistic studies by Lloyd–Jones showed that hydrogen bonding of the ligand amide N–H to the carbonyl group of the leaving group activates the allylic ester, which is crucial for the selectivity of the reaction [39]. This clearly illustrates that successful ligand design can be achieved even when it is founded on an imperfect or incomplete mechanistic basis.

The ligand size seems to be a dominant factor in the palladium-catalysed Heck reaction, as bulky phosphines [40], phosphites [41] and phosphoramidites [42] were found to lead to highly effective catalysts. For the most efficient phosphoramidite, it was shown that the steric congestion of the ligand led to mono-ligated complexes, which are more prone to substrate coordination than bis-ligated complexes. This effect had been observed before in rhodium-catalysed hydroformylation using bulky phosphite ligands (Figure 1.5) [43,44].

Hydroformylation of alkenes is a reaction that is extremely sensitive to ligand effects as well as to specific reaction conditions. Since Shell reported the beneficial use of alkylphosphines in cobalt-catalysed hydroformylation [45], many industries started applying phosphine ligands in the rhodium process as well [46]. While strongly σ -donating alkylphosphines are the ligands of choice for cobalt, they lead to low reaction rates when applied in rhodium catalysis. The application of arylphosphines reported by Wilkinson in the mid-1960s resulted in very active rhodium catalysts under very mild conditions [19].

The discovery of the rhodium triphenylphosphine hydroformylation catalysts was the basis for several industrial processes developed by Celanese (1974), Union Carbide Corporation (1976) and Mitsubishi Chemical Corporation (1978), all using this catalyst system. The UCC (now Dow Chemical) method has been licensed to many other users and it is often referred to as the low-pressure oxo (LPO) process. Major advantages of the rhodium catalysts over the cobalt ones are the higher activities, which are translated into milder reaction conditions, and higher product selectivities, resulting in better feedstock utilization. A drawback of the rhodium phosphine catalysts is the low reactivity for internal alkenes, rendering them unsuitable for higher alkene feedstocks, which are used for detergent alcohol production.

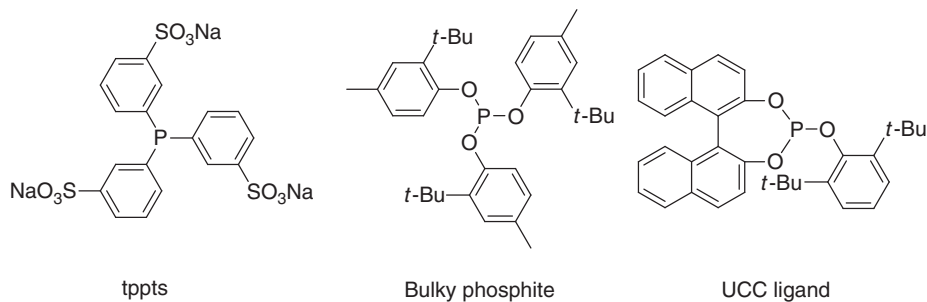


Figure 1.5 Structures of *tppts*, van Leeuwen's 'bulky phosphite' and a highly stable, bulky phosphite from UCC.

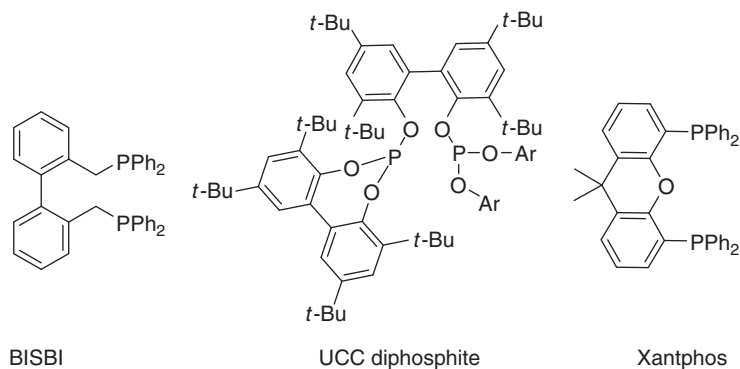


Figure 1.6 Eastman's *BISBI*, typical diphosphite from Union Carbide Corporation, and *Xantphos*.

An elegant solution for the catalyst separation problem is provided in the Ruhrchemie–RhônePoulenc process that utilises a two-phase system containing water-soluble rhodium-*tppts* (Figure 1.5) in the aqueous phase and the product butanal in the organic phase. The process has been in operation in Oberhausen since 1984 by Ruhrchemie (Celanese).

Almost two decades after the initial report by Pruet and Smith [23], a renewed interest in phosphites as ligands in the hydroformylation reaction was triggered after van Leeuwen and Roobeek reported that very high rates could be obtained by applying bulky monophosphites [44]. Bryant and coworkers at Union Carbide improved this system further by making more stable bulky monophosphites [47]. The high reaction rates were obtained at the expense of a reduced chemoselectivity due to the formation of unwanted isomerised alkenes and branched aldehydes. By changing to chelating diphosphites (Figure 1.6), they succeeded in combining very high linearities with still higher reaction rates compared to the triphenylphosphine system [48]. The 'bulky monophosphite' is applied commercially in a small-scale operation for the hydroformylation of 3-methylbut-3-en-1-ol by Kuraray [49].

Following up on the improved performance of diphosphites, diphosphines also experienced a renewed interest in the rhodium-catalysed hydroformylation. Casey and co-workers reported that the chelate angle of bidentate diphosphines affected the regioselectivity of the rhodium-catalysed hydroformylation of 1-alkenes dramatically [50]. They reported that a ligand developed by workers at Eastman, 2,2'-bis((diphenylphosphino) methyl)-1,1'-biphenyl (*BISBI*; Figure 1.6), coordinated preferentially in a bis-equatorial fashion in the trigonal bipyramidal resting state of the catalyst. This resulted in a linear-to-branched aldehyde ratio as high as 66:1 compared to a ratio of only 2:1 for equatorially-apically coordinating *dppe* (1,2-bis(diphenylphosphino)ethane).

Applying the modelling methodology developed by Casey and Whiteker [51], van Leeuwen and Kamer started a search for organic backbones for diphosphine ligands that would enforce coordination modes in between *cis* and *trans* coordination, leading to the new series of Xantphos ligands (Figure 1.6) [52]. Their studies showed that the ligand-induced bite angle had a distinct effect not only on the selectivity and activity of the rhodium hydroformylation catalyst but also in several other reactions such as the hydrocyanation of alkenes and cross-coupling reactions [53].

1.2 Properties of phosphorus ligands

The key role of phosphorus(III) ligands in late-transition metal catalysis has prompted many attempts to quantify the factors that influence the bonding of phosphorus donor ligands to transition metals and the reactivity of the complexes. For monodentate phosphine ligands, metal–ligand bonding is affected by both the electronic and the steric properties of the ligand. In order to rationalise the reactivity of transition metal–phosphine complexes, several quantitative ligand parameters have been developed. The quantitative and qualitative understanding of these ligand parameters is central to a rational design methodology, which considers their effect upon metal–ligand and ligand–substrate interactions retroactively. Moreover, these parameters have been used in linear free-energy relationships with the aim of predicting the physical properties and catalytic activity of new phosphine transition metal complexes. Unfortunately, this has proven to be less straightforward than one might expect. In order to rationalise catalytic results as functions of the ligand structures, structure–activity relationships usually explore small families of ligands which ideally vary only in a single ligand variable, such as bite angle size, steric bulk, electronic contribution and so on. Intrinsically it is difficult to affect one such parameter without affecting others; nonetheless the quantification and manipulation of ligand parameters are undoubtedly principal tools in structure–activity relationship analysis and the design of new ligands.

1.2.1 Electronic ligand parameters

The overall electronic properties of phosphorus(III) ligands have been studied using a variety of methods. One approach is to use mixed ligand complexes and assess the response of the other ligands upon electronic changes at the metal centre caused by the phosphine ligand. Strohmeier already showed that the IR carbonyl frequencies of metal complexes were a measure of the electronic properties of ligands [54]. Measuring the stretching frequencies of coordinated carbonyl ligands in transition metal complexes has become the most common way to assess the electronic effects of phosphorus ligands [55,56]. Tolman defined an electronic parameter (χ) for phosphorus ligands based on IR spectra of $\text{NiL}(\text{CO})_3$ complexes, using $\text{P}(\text{t-Bu})_3$ as a reference ligand [55]. The χ parameter of differently substituted phosphorus ligands is defined as the difference between the A_1 stretching frequencies of $\text{LNi}(\text{CO})_3$ and $\text{P}(\text{t-Bu})_3\text{Ni}(\text{CO})_3$ in cm^{-1} . Tolman showed that individual contributions of the substituents are often additive (i.e. the overall χ -value of a ligand can be taken as the sum of the χ_i -values of the individual substituents).

This approach leads to a measure of the overall electronic-donating ability of the phosphine. However, it is often necessary to consider the electronic properties of phosphines as arising from two contributions, σ -donation and π -acidity. σ -Donation is the effective dative electron donation of the phosphorus lone pair towards empty metal orbitals, whilst π -acidity refers to the acceptance (back donation) of electron density from filled metal orbitals to empty ligand orbitals (Figure 1.7). Which empty ligand orbitals are involved in back donation is still a matter of debate, but the current prevailing view is that back donation occurs from the metal d-orbitals into the σ^* -orbitals of the phosphorus ligand [57].

The separation of these two entwined electronic parameters is not trivial, and several studies have been devoted to this. One way to measure the σ -donation is via the Brønsted acidity of phosphonium salts, as

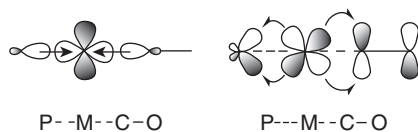


Figure 1.7 σ -donation (left) and π -back donation (right) contributions to the metal–ligand bond.

protons are not capable to participate in π -back donation and, therefore, the electron-donating potential of phosphorus can be estimated via their pK_a values. Although the interaction between the phosphorus ligand and the hard acid H^+ is very different from the interaction between the phosphorus ligand and a soft transition metal complex, a number of organometallic reactions do show a linear relationship between pK_a values of phosphorus ligands and the $\log k$ of the reaction. Considering the extreme sensitivity of the pK_a values of phosphorus bases to solvation energies, these good correlations are remarkable.

Drago postulated that σ -donation itself may be more complicated and should be defined by two parameters E_B and C_B , representing electrostatic and covalent contributions to the phosphine reactivity [58,59]. Drago's model is based on the enthalpies of adduct formation between a phosphorus σ -donor and a number of different π -acceptors, measured in poorly solvating solvents, which are used to quantify the σ -donating property of a phosphine donor. However, this method showed significant steric and π -acidity effects for bulky acceptor ligands [59].

The development of a quantitative measure for the π -acidity of phosphorus ligands has also proven to be difficult. Graham and Treichel discussed almost simultaneously the use of CO-stretching frequencies in octahedral $\text{LM}(\text{CO})_5$ complexes for separation of the σ -donation and π -back donation contributions to the metal–ligand bond [60]. They reasoned that the π -acceptor capacity of ligand L should mainly affect the stretching frequency of the *trans*-coordinated carbon monoxide ligand by competing for the electron density of metal d-orbitals of the correct symmetry that are used in the M–CO back donation (Figure 1.7). In contrast, the σ -donating property of ligand L would affect the stretching frequencies of both the *cis*- and *trans*-coordinated carbon monoxide ligands in a similar fashion. Unfortunately, the method proved to be not very straightforward, as it predicted, for instance, that tributylphosphine is more π -acidic than triphenylphosphine.

One of the most comprehensive studies of ligand effects, known as quantitative analysis of ligand effects (QALE), was described by Giering and Poe [61]. The QALE model is based on the analysis of several physical properties of metal complexes: ν_{CO} for $(\eta^5\text{-cp})(\text{CO})(\text{L})\text{Fe}(\text{COMe})$, E^0 and H^0 for the $(\eta^5\text{-cp})(\text{CO})(\text{L})\text{Fe}(\text{COMe})^{+/0}$ couple, the pK_a value of HPR_3^+ and the ionisation energy of PR_3 . Giering showed that the electronic properties of a ligand should be described by three instead of two electronic parameters: their σ -donor capacity (χ_d), π -acidity (π_p) and an aryl effect (E_{ar}). This last parameter is now believed to be more fundamental and not limited to aryl-containing phosphines, but its physical meaning is still unclear [61].

Computational methods offer an excellent platform to study electronic effects in metal–phosphorus bonding in individual complexes and in some catalytic reactions [62,63]. The effects of σ -donation and π -back donation in transition metal complexes can be distinguished on the basis of the symmetry of the orbitals involved in the metal–phosphorus bonding. Pacchioni *et al.* studied the metal– PR_3 interaction in several palladium complexes and found only minor variations in the σ -donor strength of PR_3 ligands, while large differences in π -acidity were observed [64]. Computational studies by Branchadell and co-workers revealed similar behaviour in $\text{Fe}(\text{CO})_4\text{PR}_3$ complexes [65]. Based on these results, they proposed to divide ligands into pure σ -donor ligands and σ -donor– π -acceptor ligands. Landis *et al.* studied the bond dissociation energies in rhodium–phosphine complexes and showed that the relative importance of σ -donation and π -back donation in the metal–phosphorus bond is highly dependent on the other ligands coordinated to the metal [66]. Landis argued that this σ – π synergy leads to very subtle effects at the metal centre, which makes prediction of ligand effects *a priori* difficult.

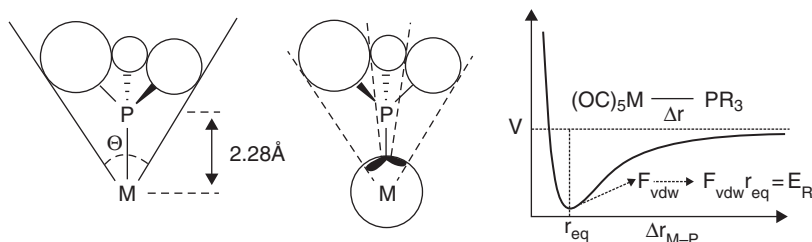


Figure 1.8 Tolman's definition of the cone angle (left), White's definition of the solid angle (middle) and Brown's definition of E_R .

1.2.2 Steric ligand parameters

Complementary to the development of reliable electronic parameters, several steric parameters have been introduced. One of the most widely applied concepts for quantifying the steric bulk of monophosphines is the cone angle (θ) (Figure 1.8), which was introduced by Tolman [18]. From a metal centre located 2.28\AA from the phosphorus atom of the ligand (a typical Ni–P bond distance), a cone that embraces all the atoms in the ligand based on CPK models is constructed (Figure 1.8). The resulting cone angle θ is a measure for the steric bulk of a ligand. Unfortunately, ligands rarely form a perfect cone and multiple ligands coordinated to one metal centre can mesh, creating less steric bulk around the metal than would be expected based on the sum of their individual cone angles. In many square-planar complexes, the sum of the individual cone angles is found to be much more than the available 360° . The increasing use of computational methods has resulted in several more elaborate approaches to alleviate these shortcomings [67]. White *et al.* introduced the concept of solid angles [68]. Based on either crystal structures or calculated structures, the van der Waals radii of the ligand atoms are projected onto the van der Waals surface of the metal centre (Figure 1.8). The amount of coverage, given by the solid angle, is a measure of the steric bulk around the metal.

Most measures for steric bulk are geometric in nature, but the actual physical meaning of steric congestion is a repulsive energy induced between different ligands in a transition metal complex. Brown *et al.* defined a steric repulsive energy parameter, E_R , that is based on a molecular mechanics computational model of $\text{LCr}(\text{CO})_5$ [67,69]. The van der Waals repulsive force between the metal complex and the ligand (F_{vdw}) is calculated starting from the optimised structure of $\text{LCr}(\text{CO})_5$ by varying the Cr–L distance. E_R is defined as the product of this van der Waals repulsive force and the metal–ligand bond distance (Figure 1.8). This method has a distinct advantage over the purely ligand-based methods as the conformation of the ligand corresponds better to the real conformation of the ligand in transition metal complexes. A drawback is that intimate knowledge of all force constants of the complex is required.

Barron *et al.* developed another semiquantitative approach to describe the steric properties of bidentate ligands. The ‘pocket angle’ concept is based on X-ray crystal structure data of palladium(II)–diphosphine complexes and estimates the size of the active site at palladium by calculating the interior cone angle of the bidentate ligand [70].

Leitner *et al.* proposed the ‘accessible molecular surface’ as an alternative approach based on molecular modelling to describe the interplay between the PR_2 fragment and the metal. The accessible molecular surface is determined by calculating the conformational space of the active fragment (i.e. [(P–P)Rh]). These conformations are then superimposed to provide a ‘pseudo-dynamic’ structure which can be visually interpreted for qualitative understanding or quantified by AMS analysis [71]. This method requires substantial knowledge of force-field parameters, but in this case these could be obtained from X-ray crystallographic data.

In recent years, the development of new powerful computational techniques has enabled the calculation of larger catalytic systems and the detailed study of steric effects in catalysis [72]. Although most catalyst

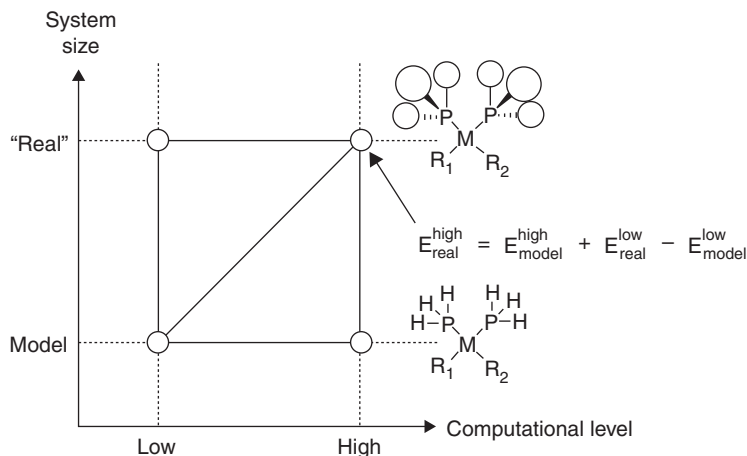


Figure 1.9 General computational scheme for the calculation of large molecular systems.

systems are still too large for the use of accurate, high-level *ab initio*- or density functional theory-based methods, the new techniques allow the separation of the catalytic complex into a reactive centre and a non-reactive periphery (Figure 1.9). While the reactive centre is treated at a high level of theory, the nonreactive periphery, which is mostly responsible for steric effects, is treated at a lower (and therefore less costly) level of theory. This also allows the straightforward separation of steric and electronic effects. These techniques have now been used to calculate key transition metal complexes, as well as determine pure steric effects in some catalytic processes such as the hydrogenation of enamides [73,74], the hydroboration of arenes [75], the hydroformylation of alkenes [76], the hydrosilylation of alkenes [77], the cyclodimerisation of 1,3-butadiene [62] and early- and late-transition metal-catalysed olefin polymerisation reactions [78]. One of the most important conclusions from these calculations is that not only is the amount of steric bulk important, but also the geometrical placement of the bulk around the metal centre can have a dramatic influence on the activity and selectivity of transition metal complexes in catalysis.

1.2.3 Bite angle effects

Bidentate phosphine ligands have found wide application in catalytic reactions since they can lead to increased stability and often an increased regio- and stereoselectivity of the catalyst system. The chelating effect of bidentate ligands reduces the tendency for ligand dissociation during the catalytic cycle, resulting in better defined catalytic species under catalytic conditions. Classification of bidentate ligands with the use of Tolman's electronic and steric parameters has proven to be difficult. Next to the traditional steric and electronic effects caused by the substituents at the phosphorus centre in monodentate ligands, the phosphorus-phosphorus distance in bidentate ligands, induced by the ligand backbone, proved to be an important ligand parameter [79,80].

To be able to quantify the effect of strain imposed by bidentate phosphine ligands, Casey and co-workers developed the concept of the natural bite angle [51]. This ligand parameter is based on simple molecular mechanics simulations. Similar to Tolman's cone angle concept, a dummy metal atom is introduced that coordinates to both phosphorus donor atoms at a distance of 2.315 Å. The function of this dummy metal is to ensure that bidentate coordination is preserved by allowing only ligand geometries in which the donor atoms have the proper orientation. In order to exclude contributions of the metal to the P-M-P angle, the P-M-P force constant is set to zero during geometry optimisation. The result is a purely ligand-induced P-M-P

angle that can be used to compare different bidentate ligands. These calculations require prior knowledge of the remaining force constants in the metal complex, including force constants describing M–P stretching, M–P–X bending, dihedral bending and torsional deformations. These are often ignored, and changes in these parameters may cause large differences in the calculated natural bite angles. Despite this, the natural bite angle parameter has been correlated successfully with bite angle effects in a number of reactions involving transition metal complexes, including industrially important processes such as rhodium-catalysed hydroformylation, nickel-catalysed hydrocyanation and palladium-catalysed alkoxy- and hydroxycarbonylation.

The bite angle of the diphosphine ligand affects the properties of the metal complex in two fundamentally different ways; via an electronic effect on the metal complex and via the steric bulk induced by the ligand [79,81]. While in some reactions the electronic effect seems dominant, in other reactions the steric bulk of the bidentate ligand determines the overall bite angle effect. In many reactions, however, the physical origin of the observed overall bite angle effect remains unclear. Especially when multiple reaction steps in the catalytic cycle are affected by the bite angle of the bidentate ligands, rationalisation of the observed (overall) effect can be difficult. Clearly, separation of electronic and steric bite angle effects in catalytic reactions would increase our understanding of transition metal-catalysed reactions and allow for rational design of new catalyst systems.

1.2.3.1 Electronic bite angle effect

The term *electronic bite angle effect* refers to the electronic changes at the metal centre as a function of the natural bite angle of the bidentate ligand. Dierkes *et al.* introduced the concept of metal-preferred bite angle [79]. The *metal-preferred bite angle* is defined as the lowest energy P–M–P angle of the metal complex in the absence of steric effects. The better the ligand's natural bite angle matches this metal-preferred angle, the better the ligand is able to stabilise the metal complex. In a rough approximation, ligands exhibiting a natural bite angle of around 90° stabilise square planar and octahedral complexes, ligands exhibiting a natural bite angle of around 109° stabilise tetrahedral complexes and ligands exhibiting natural bite angles around 120° stabilise trigonal bipyramidal complexes. However, other ligands coordinated to the metal do affect the metal-preferred bite angle. More accurate metal-preferred bite angles can be obtained from *ab initio* and density functional theory (DFT) calculations on model complexes, which also allow the determination of metal-preferred bite angles of transition states.

Deviations of the metal-preferred bite angle of a complex induced by a bidentate ligand lead to electronic destabilisation of the metal complex and consequently to different reactivity. Especially in reactions where the geometry at the metal centre changes during the reaction, large differences in the reactivity and relative thermodynamic stability of the reaction intermediates are observed. Figure 1.10 depicts the orbital changes associated with the change of the L–Pt–L angle in the PtL₂ fragment [82]. For Pt(0), all d-orbitals at the metal centre are filled and the optimal orbital stabilisation is obtained for a L–Pt–L angle of 180°. For Pt(II), only four d-orbitals are filled, resulting in an empty $\delta_g^*/2b_1$ orbital. Consequently optimal stabilisation for the Pt(II) centre is obtained for a L–Pt–L angle of 90°.

Theoretical methods have been used to investigate electronic bite angle effects in several transition metal-mediated reactions. Thorn and Hoffman used extended Hückel calculations to show that, for hydride migration to a platinum-coordinated alkene, the bite angle of the spectator diphosphine ligand increases from 95° in the reactant to 110° in the transition state [29]. They argued that ligands with a natural bite angle of around 110° stabilise the transition state and destabilise the ground state and consequently accelerate the reaction. Indeed, a β -agostic intermediate between an alkene–hydride and an alkyl structure was observed for PtH(ethene)(dppp-Bu), which in the solid state showed a P–M–P angle of around 105°. The corresponding PtH(ethene)(dppe-Bu) complex, exhibiting a smaller bite angle of 90°, did not show this β -agostic intermediate.

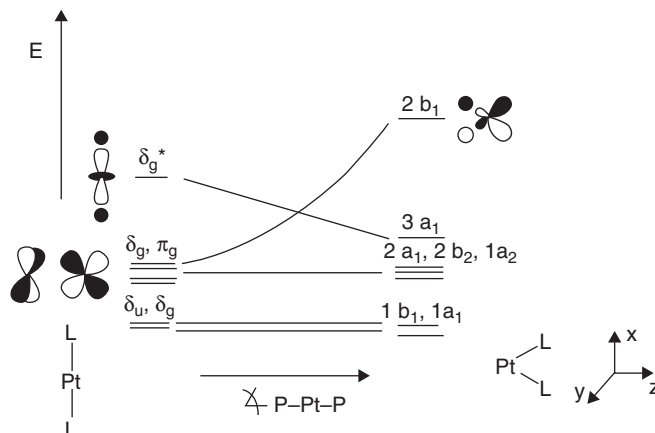


Figure 1.10 Electronic bite angle effect in platinum complexes containing a predominantly σ -donor bidentate ligand [82]. Reprinted from S. Otsuka, 1980 with permission of Elsevier.

Electronic bite angle effects have also been observed in other experimental studies. Dubois and co-workers found a decrease of the half-wave potentials of Ni(II/I) and Pd(II/0) couples in square planar $M(\text{diphosphine})_2(\text{BF}_4)_2$ with an increase of the natural bite angle of the ligand [83]. Similarly, both the hydride donor strength and pKa of $\text{HM}(\text{diphosphine})_2\text{X}$ ($M = \text{Ni}, \text{Pd}, \text{Pt}$) decrease as the natural bite angle of the diphosphine ligand increases [84]. Both observations were attributed to a larger tetrahedral distortion of the reduced product for large bite angle ligands. Also, Angelici observed that the basicity of trigonal bipyramidal $\text{Fe}(\text{diphosphine})(\text{CO})_3$ decreases as the bite angle of the diphosphine ligand increases [85], large bite angle ligands favouring the trigonal bipyramidal geometry of the reactant complex over the octahedral geometry of the protonated product.

1.2.3.2 Steric bite angle effect

The steric bite angle effect is based on the change in steric interactions around the metal complex when the backbone of the bidentate ligand is modified, while keeping the substituents at the donor atoms constant. Since ligand–ligand and ligand–substrate interactions influence the relative energies of stable intermediates and transition states of the catalytic cycle, the change in bite angle has a direct influence on the activity and regioselectivity of the catalytic system (Figure 1.11).

Purely steric bite angle effects in catalysis are uncommon. Recently, we argued that the observed bite angle effect on the regioselectivity of the rhodium–diphosphine catalysed hydroformylation of alkenes, and the product selectivity in the CO–ethylene copolymerisation is largely steric in origin [81]. In the allylic alkylation reaction, both the regio- [86] and stereoselectivity [38,87] of the reaction are influenced by the steric properties of the bidentate ligands. The origin of both effects was attributed to the increased embracing of the metal by wide bite angle ligands. It should be noted that in this reaction also significant electronic effects were observed.

1.2.3.3 Steric versus electronic bite angle effects

Rational catalyst design relies on proper understanding of individual steps during a catalytic cycle. This process can be complicated, however, as each step will contain an associated transition state which cannot be observed directly. Therefore, investigating steric and electronic contributions to the transition state is often

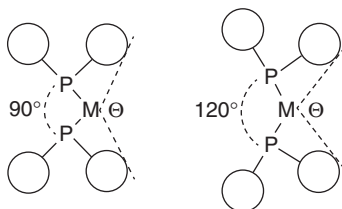


Figure 1.11 Steric bite angle effect. θ represents the pocket angle, as defined by Barron and co-workers [70].

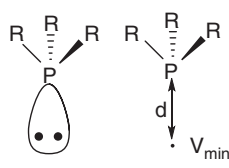
approached computationally. Bickelhaupt *et al.* [88] have attempted to distinguish between steric and electronic bite angle effects on the oxidative addition of $\text{CH}_3\text{-X}$ (where $\text{X}=\text{H}$, CH_3 and Cl) to palladium complexes with a series of bridged primary diphosphine ligands of the general structure $\text{PH}_2(\text{CH}_2)_n\text{PH}_2$ (where $n=1\text{--}6$) by performing DFT calculations. For comparison, the diphosphine complex $\text{Pd}(\text{PH}_3)_2$ was included in the study. They examined the strain energies of deformation experienced by both the catalyst and the substrate upon coordination and oxidative addition, the substrate–catalyst interaction energy, and the transition state bite and twist angles. Bickelhaupt *et al.* suggested that ligands enforcing narrow bite angles could alleviate steric interactions and lower the activation barrier, thereby essentially activating the metal complex to oxidative addition [88] (i.e. the bite angle effect is steric in nature). However, experimental studies by the group of van Leeuwen *et al.* revealed both steric and electronic effects on the activity of nickel-catalysed hydrocyanation of styrene [89,90]. These ligands were designed to activate the catalyst to undergo reductive elimination (the reverse of oxidative addition). Bickelhaupt's assertion would predict that a larger bite angle would give a higher activity for the reductive elimination. However, the observation was that the system had an optimum activity at a ligand bite angle of $105\text{--}106^\circ$ with a loss in activity as the bite angle was further increased to 109° [89]. DFT calculations on the reductive elimination of alkyl cyanides from palladium–diphosphine complexes revealed that ligands favouring a bite angle of $105\text{--}106^\circ$ optimally stabilise the transition state structure while destabilizing the square planar reactant [91]. This effect was observed for both methyl- and phenyl-substituted diphosphines, ligands with different steric properties. QM–MM calculations showed that the bite angle effect could be reproduced only if the electronic influences of the substituents at phosphorus were accounted for, demonstrating that for these ligands in this reaction the electronic bite angle effect dominates. Moreover, experimental studies showed that electron-withdrawing ligands further enhanced catalyst activity for a series of ligands with an effectively constant bite angle [90]. Therefore, evidence suggests that the bite angle effect is not solely steric in origin and does include electronic and orbital contributions, at least for Ni-catalysed hydrocyanation.

1.2.4 Molecular electrostatic potential (MESP) approach

The parameters for steric and electronic properties described until now are based on experimental data. Actual prediction of the properties of newly designed ligands would be very advantageous [92]. The use of molecular electrostatic potential (MESP) for the simultaneous evaluation of steric and electronic properties of phosphines was recently investigated by Suresh *et al.* [93,94].

The MESP approach was used to calculate the most negatively charged point in the lone pair region (i.e. the global minimum). The MESP is a physical property that can be determined either experimentally (by X-ray diffraction) or computationally from the electron density distribution ($\rho(r)$) (see Figure 1.12; Z_A is the charge of nucleus A located at R_A). Normally, lone pair regions on a molecule show minimum values of V due to a larger value of the electronic term in the equation as compared to the nuclear term.

MESP is defined as the energy required to bring a unit test positive charge from infinite to r . V_{\min} points represent centres of negative charge on a molecule, and could be related to the 'location' of the lone pairs

$$V(r) = \sum_A^N \frac{Z_A}{|r-R_A|} - \int \frac{\rho(r') d^3 r'}{|r-r'|}$$


R	V_{\min} (kcal/mol)	d (Å)
H	-28.22	1.850
Cy	-44.49	1.741
Ph	-34.85	1.816

Figure 1.12 Calculation of the minimum electrostatic potential (V_{\min}).

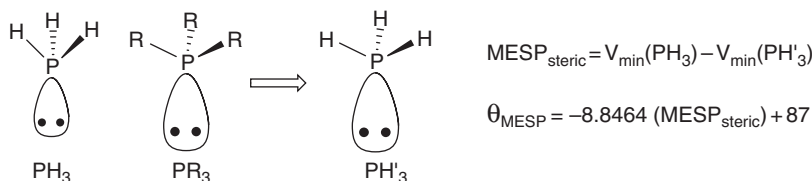


Figure 1.13 Schematic representation of the approach used to calculate $\text{MESP}_{\text{steric}}$ and the associated cone angle (θ_{MESP}).

(Figure 1.13). The value of V_{\min} is a quantitative measure of the ‘lone pair strength’, and consequently of the electron-donating properties of the phosphine [93]. The accuracy of this measure was proved by obtaining acceptable linear correlations with previously defined electronic parameters as $\text{p}K_a$, $\nu(\text{CO})$, ΔE , ΔH° and E .

The V_{\min} obtained by the MESP approach is inherently dependent on the steric properties of the ligand as well; the bulkier the substituents, the wider the R–P–R angle, and consequently the more p-character on the sp^3 -hybridised lone pair orbital. This subtle change is reflected in an increased Lewis basicity of the phosphine and absolute value of V_{\min} .

This fact can be used to evaluate steric parameters by a two-layer calculation, similar to the approach depicted in Figure 1.9. The intervalence R–P–R bond angles of the PR_3 ligand are determined by optimising the ligand structures using molecular mechanics (MM) calculations employing a universal force field. In the model, the R groups, representing the outer layer of the model, are connected to the P via imaginary link H atoms. These H atoms define an inner layer consisting of a PH_3 ligand, which is optimised sterically by the MM calculation as if H were the R group. The thus obtained (sterically influenced) optimal geometry of the inner layer is then evaluated using DFT calculations to determine V_{\min} . The difference between this V_{\min} and that of a fully optimised PH_3 structure is defined as the $\text{MESP}_{\text{steric}}$ parameter (i.e. the steric effect of R on the ligands electronic properties) (Figure 1.13).

A linear correlation was found between this parameter ($\text{MESP}_{\text{steric}}$) and Tolman’s cone angle, and from this correlation, a new steric parameter (θ_{MESP}) can be defined. This methodology constitutes *the first quantum mechanically derived electronic quantity that interpreted the cone angle data* [94].

Fey and Harvey *et al.* [95,96] have recently approached the problem by developing ligand knowledge bases using DFT calculated ligand and ligand complex descriptors, including, but not limited to, descriptors for electronic properties (e.g. frontier molecular orbital energies and proton affinities), steric properties (e.g. bite angles and He_8 -wedges) and other chemically relevant information such as metal–ligand bond lengths and changes in ligand geometry upon complexation [96]; the authors used their calculated descriptors to produce the first map of ligand space for bidentate ligands via principal component analysis (PCA). This approach to visualise correlations between ligand descriptors is useful but limited in its ability to quantitatively analyse ligand sets. Nevertheless such maps can prove very useful in qualitative analysis of ligand clustering, identifying ligand similarities and perhaps aiding in intuitive ligand design.

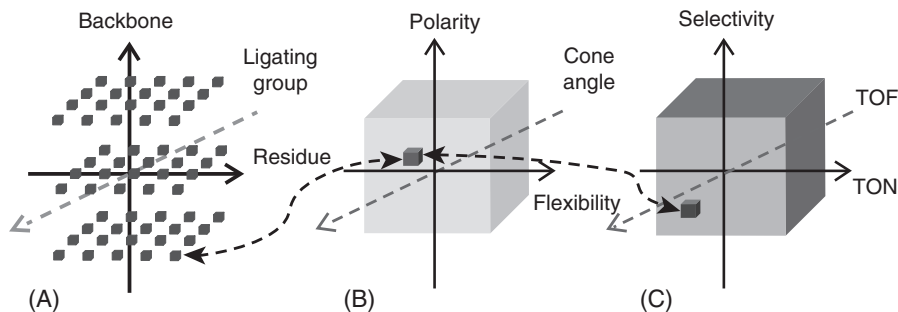


Figure 1.14 Simplified representation of the three multidimensional spaces A, B, and C. Reprinted from A. Maldonado, et al., 2009 with permission of Wiley-VCH Verlag GmbH & Co. KGaA.

Consequently, the authors have successfully demonstrated a computational approach to describing ligand properties in a computationally, chemically and statistically robust way. Currently, the limitation of such an approach, even by the authors' own admission, is in the availability of experimental data to test and challenge the calculated models and maps. However, they are optimistic that more even and extensive sampling of ligand structures, especially of more exotic systems and not just alkyl-aryl phosphines, could improve reliability and the predictive power of such maps, thus providing a valuable tool for ligand design and catalyst discovery [95,96].

Recently they reported an interesting application of their computational approach in which they detected fluorophosphines as promising ligands for rhodium-catalysed hydroformylation of alkenes [97]. This unexplored class of ligands was found to be close to phosphites in ligand space in their computational studies and indeed showed good performance in this catalytic reaction. This nicely illustrates that computational methods can have predictive power, leading to a new class of potentially useful ligands that probably would not have been explored otherwise.

Rothenberg and co-workers have developed another approach, which they called *in silico design*, aiming at identifying new active catalysts [98–102]. Instead of trying to understand ligand parameter control, they attempt to derive quantitative structure–activity relationships based upon topological descriptors, using a virtual library of known ligands in a multidimensional approach consisting of three spaces (Figure 1.14). Space A contains a library of catalysts, space B contains the catalyst and reaction descriptors (e.g. backbone flexibility and temperature) and space C contains figures of merit such as measures of catalyst performance (e.g. TON, TOF and ee), and also real-world concerns such as cost.

The relationships between B and C are quantified using quantitative structure–activity relationship (QSAR) and quantitative structure–property relationship (QSPR) models. New catalyst designs based on this computational method may be achieved using the validated model. Depending upon the size of the virtual library, millions of catalysts can be screened *in silico*, which could lead to new particularly interesting catalyst structures.

1.3 Asymmetric ligands

The use of chiral phosphine ligands for asymmetric catalysis has seen a spectacular growth in recent decades. The development of better asymmetric catalysts has been driven by the industrial need for enantiopure compounds that are not available in the chiral pool, and the costs and difficulties associated with the resolution of racemates. From the first report in 1968 by Knowles and Sabacky [103] on asymmetric hydrogenation using a known chiral phosphine (–)PMePh(*i*-Pr), a plethora of chiral mono- and diphosphines have appeared in the literature. Some early outstanding examples are shown in Figure 1.15 [7,104].

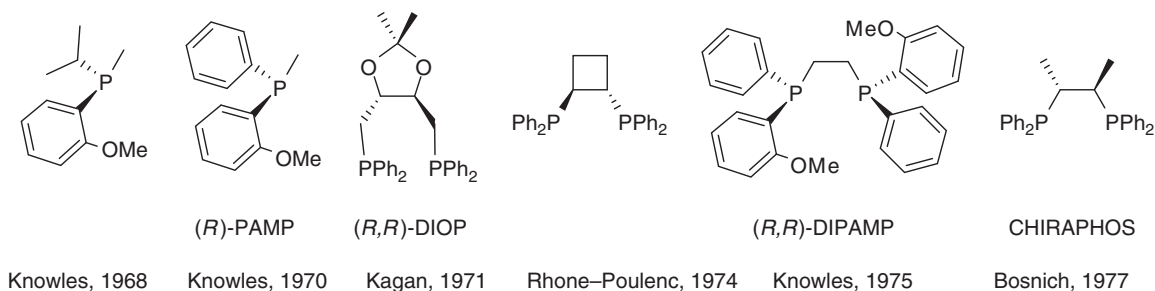


Figure 1.15 Some chiral mono- and diphosphines relevant to asymmetric hydrogenation.

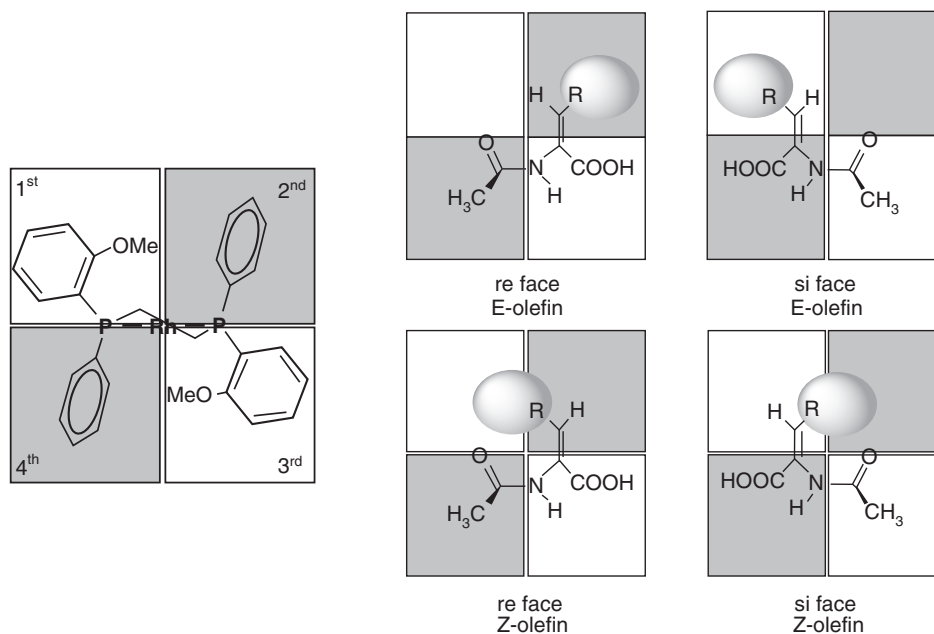


Figure 1.16 Quadrants model for Rh -(R,R)-DIPAMP.

In particular, chelating diphosphine ligands provided efficient catalysts for the hydrogenation of *Z*-enamides to form α -amino acids with high enantioselectivities (over 95% ee). Already in the early days, it was noted that all these ligands create a C_2 -symmetric environment around the metal centre when coordinating to a square planar rhodium complex. In the case of DIPAMP, the X-ray structure of the catalyst precursor $[Rh(DIPAMP)(diene)]^+$ showed that enantioselectivity is achieved thanks to a restrained disposition of the phenyl groups, two of them being face exposed and the other two edge exposed (see Figure 1.16). A similar orientation is taken by other C_2 -symmetric diphosphines, which have stereogenic centres on the backbone rather than on the phosphorus. This special arrangement divides the space available for substrate coordination into “four quadrants” of which two are closer to edge-exposed phenyls (second and fourth) and consequently more hindered than the ones which are closer to face-exposed phenyls (first and third). Coordination of the enamide to the metal centre takes place via the substituted alkene and the carbonyl oxygen as an additional donor atom. The preferred coordination face of the alkene (*re* or *si*, for short) will be the one that minimises the steric interaction with the phenyls of the ligand. The importance of steric interactions was soon

corroborated by the observation that Z-enamides were more efficiently hydrogenated (faster and with higher ee) than E-enamides [105].

Although a direct correlation of the major adduct formed and the stereoselection of the reaction could be attractive, detailed studies by Halpern [106] and Brown [107] proved that the major enantiomeric product does not derive from the most stable of the alkene adducts. In fact, the less stable intermediate alkene complex reacts faster in the subsequent reactions, showing the so called *anti-lock-and-key* behaviour.

This early example established the first attempted rationalization of the relationship between ‘chirality of the ligand’ and asymmetric induction. Although the final understanding required a better knowledge of the specific reaction mechanism, the quadrants model constitutes nowadays a useful tool to rationalise the stereoselection observed when using many other C₂-symmetric ligands (some examples are cited in [74,108]). Historically, it has been accepted that C₂-symmetric ligands that effectively create a chiral environment around the metal centre are most efficient in asymmetric catalysis and consequently this kind of ligand has proliferated enormously in recent decades.

The quadrant model is a qualitative descriptor based on steric encumbrance. It intrinsically does not provide any quantitative predictions of enantioselectivity, but merely predicts the sign of the stereochemical outcome. Recently, the quadrants model has also been applied to describe the chiral environment created for some C₁-symmetric diphosphines [109], which effectively block three of the four quadrants by the substituents of the phosphorus atom (Figure 1.17). Also several C₁-symmetric phosphines have been very successful in many catalytic reactions. In most of the cases, not only steric but also electronic factors play a key role in the enantiodiscrimination [10,110].

Although the quadrants model is a very intuitive method based on simple symmetry principles, it is still one of the few successful tools used to design a chiral diphosphine. Nevertheless, several new methods are being developed by theoretical groups in the last years in an attempt to change this situation.

Similar to applying steric and electronic parameters for rational catalyst design, a parameter to quantify the chirality content of a molecule could facilitate similar design of chiral ligands and later on relate it with the enantiomeric outcome of the reaction. The definition in 1995 by Avnir of *chirality* as a continuous molecular structural property can be considered a milestone [111]. He defined a new parameter called *continuous chirality measure* (CCM, S), as shown in Figure 1.18.

Applied to molecules, P_i represent the positions of the *n* atoms on a molecule and P'_i the position that they would occupy in the ‘nearest’ achiral conformation. D is a normalization factor to make S independent of the

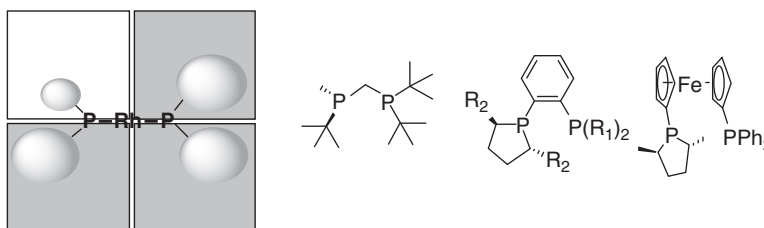


Figure 1.17 Diphosphines fulfilling the three-full-quadrants model.

$$S = \frac{100}{n D^2} \sum_{i=1}^n (P_i - P'_i)$$

Figure 1.18 Continuous chirality measure.

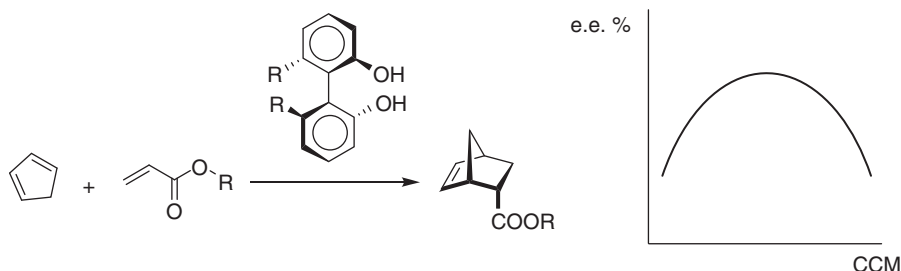


Figure 1.19 Correlation between the ee obtained and CCM value for a 2,2'-biaryldiol catalysed Diels–Alder reaction.

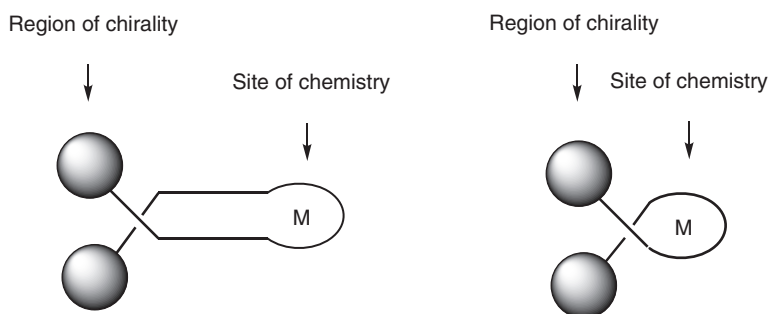


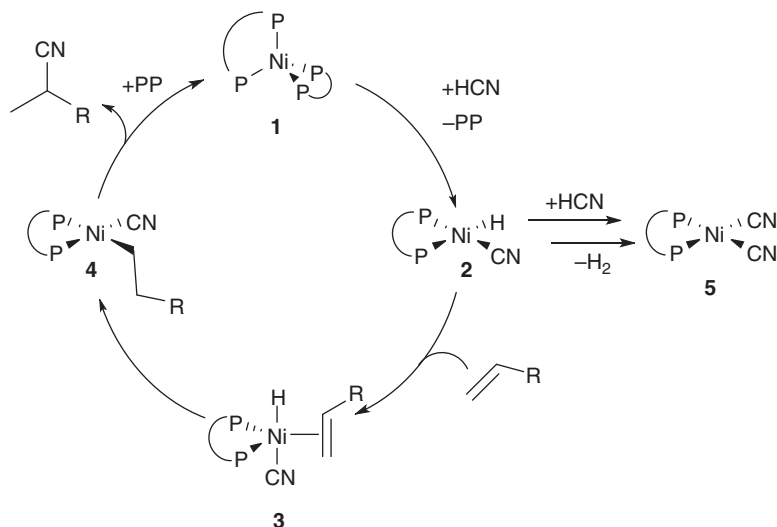
Figure 1.20 Efficient and inefficient chiral catalyst as defined by Lipkowitz.

size of the molecule. The *S* parameter varies from 0 for nonchiral molecules to 100, which is the highest possible value.

Later publications relating this new parameter with the enantiomeric excesses experimentally obtained showed encouraging success [112], but one example concerning Diels–Alder condensations catalysed by 2,2'-biaryldiols evidenced that it could not be generalised so easily [113].

They observed a nonlinear correlation between the computed CCM values and the experimental enantioselectivity. In fact, the correlation observed was basically the same as the one observed between the twist angle of the aryl rings and the ee (Figure 1.19). These results demonstrate that quantifying chirality does not automatically provide predictive power by itself, as an effective ligand should also create an asymmetric environment in the vicinity of the 'active site' of the catalyst. As formulated by Lipkowitz, 'chiral catalysts that are efficient at inducing asymmetry will have their region of maximum stereoinduction spatially congruent with the site of chemistry (bond making-breaking)'. Obviously, one of the important factors influencing asymmetric induction will be the distance between the asymmetric environment and the active site. If they are too far apart, the diastereomeric transition states will have the same or similar energies and no asymmetric induction will be observed (Figure 1.20).

In order to create a more effective methodology, Lipkowitz developed a procedure called *stereocartography* [114]. It comprises mapping of the most stereo-inducing regions around a catalyst. The calculations are done in the following manner: the centre of mass of the catalyst is placed at the centre of a Cartesian coordinates system, and a three-dimensional (3D) fine grid is defined around it. The molecule(s) reacting with it in their transition state conformation are placed sequentially at each grid point in all the possible orientations, and the intermolecular energy force is computed. The same procedure is followed for the pro-R and pro-S transition states. The results obtained for both enantiomeric transition state "substrates" are



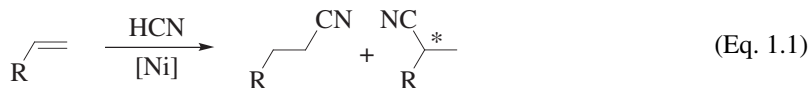
Scheme 1.1 Simplified mechanism for nickel catalysed hydrocyanation.

compared, locating the grid points of maximal energy difference which are considered as the points of maximal stereodifferentiation. Out of a set of 18 catalysts evaluated by using this methodology, 17 showed a correlation between the distance linking these maximal stereodifferentiation points to the region where the chemistry is actually taking place and the observed enantioselectivity.

1.4 Rational ligand design in nickel-catalysed hydrocyanation

1.4.1 Introduction

Despite advances in computational modelling and fundamental understanding of the influence of ligand parameters on organotransition metal chemistry, the predominant approaches to catalyst design employ a cycle of crude design, synthesis, testing and refinement of the design. Invariably, ligand design is an iterative process, building upon the performance of previous ligands and the understanding of the mechanism of the catalytic reaction. Sometimes this informed iterative approach can lead to remarkably predictable results, but on the other hand, surprising results are also often encountered. The nickel-catalysed hydrocyanation of alkenes, briefly presented here, is an example of an important catalytic reaction where detailed mechanistic knowledge and understanding have allowed for successful design of effective ligands.



Catalytic hydrocyanation (Eq. 1.1), the introduction of HCN across a double bond, was long ago established and industrialised in the well-known DuPont adiponitrile process. This process utilises a Ni/P(O-*o*-tolyl)₃/Lewis acid system. Since the commercialisation of the DuPont process, many groups have carried out detailed mechanistic studies [115–122], and Scheme 1.1 shows a simplified mechanism based on that proposed by McKinney and Roe [120,122].

1.4.2 Mechanistic insights

The catalytic cycle starts with a tetrahedral Ni(0) complex: (1) ligand dissociation followed by oxidative addition of HCN provides the intermediate square planar Ni(II) species; (2) coordination of the substrate olefin forms the intermediate trigonal bipyramidal π -olefin complex (3), which rapidly undergoes hydride migration to form the square planar σ -alkyl Ni(II) species; and (4) the final step is the reductive elimination of the product alkylnitrile and regeneration of the tetrahedral starting complex 1. A competing catalyst decomposition pathway exists when a second equivalent of HCN oxidatively adds to the square planar Ni(II) species 2, losing H₂ gas and generating a square planar biscyano Ni(II) species 5. The latter is inactive and cannot be easily regenerated.

Mechanistic studies of McKinney and Roe showed that reductive elimination is the rate-determining step in the Ni-catalysed hydrocyanation of alkenes [122]. Recent work by Vogt *et al.* showed that, also for the isomerisation of 2-methyl-3-butenitrile to 3-pentenitrile, reductive elimination was the rate-limiting step, and they observed a zero-order dependence on the substrate concentration [123]. The advantage of their study was that the reductive elimination step could be investigated without the complication of catalyst deactivation caused by HCN via the production of a bis cyano Ni species (5). Also, this model reaction facilitated the assessment of the effects of ligand parameters on the reductive elimination step.

1.4.3 Rational design

The first example of rational catalyst design for the hydrocyanation reaction was reported in the early 1990s. Pringle and co-workers explored chelating ligands with the intention to stabilise the nickel(0) complex and to reduce bis cyano complex formation, a disadvantage of the DuPont system. In order to retain similar electronic properties as the DuPont catalysts, they applied new chiral diphosphite ligands based upon bisphenol (L1) and binaphthol backbones (L2) [124,125] (Figure 1.21).

Although the 2,2'-bisphenol-based diphosphite ligand was less selective than the DuPont system for hydrocyanation of butadiene, a fourfold increase in turnover number was observed for the bidentate ligand system, and the catalyst stability was strongly enhanced [125]. Similar higher stabilities were observed for complexes of binaphthol diphosphite (L2) compared to the monodentate binaphthol phosphite (L3) and bidentate phosphines. Also much higher yields of up to 70% and ee's of up to 38% (with BPh₃ added) were

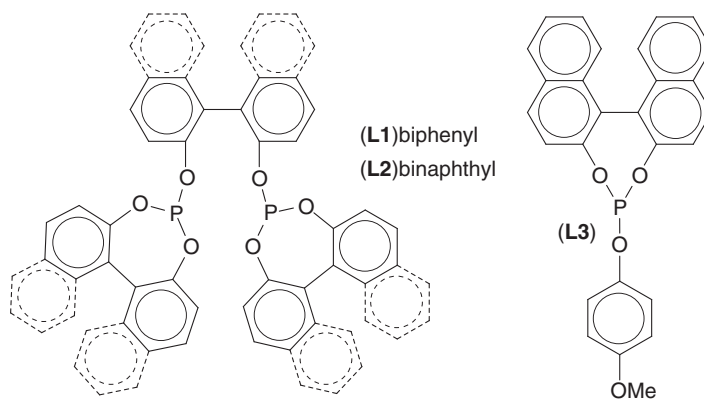


Figure 1.21 Biphenyl and binaphthyl.

observed in the hydrocyanation of norbornene using the nickel complex of ligand L2, which outperformed both the Ni–DIOP and Ni–monophosphite catalysts [124].

A further example of successful ligand design in hydrocyanation based on both mechanistic knowledge of the catalytic reaction and fundamental understanding of ligand parameters on the reactivity of metal complexes was reported by the groups of van Leeuwen and Vogt [89]. Prior to their report, application of phosphines as ligands had failed to produce results that could compete with phosphites [124]. The obvious reason is that the rate-limiting reductive elimination step is retarded by strongly σ -donating ligands such as phosphines.

The group of Kamer and van Leeuwen had prepared a series of ligands designed to enforce wide bite angles (β_n : 101–131°) (Figure 1.22), which was anticipated to destabilise the Ni(II) square planar resting state and stabilise the tetrahedral Ni(0) complex formed after reductive elimination. This was expected to compensate for the strongly donating effect of phosphines, and indeed greatly enhanced yields (up to 95%) and regioselectivities (up to 99%) compared to other diphosphines in the hydrocyanation of styrene (Table 1.1) [89]. The enhanced stabilization of the Ni(0) complexes formed after reductive elimination has a tremendous effect on the reaction rate, which is clearly illustrated in Figure 1.23, depicting a plot of the yield of hydrocyanation product versus the calculated natural bite angle.

The electronic ligand effects were further explored by testing a series of electronically tuned Thixantphos ligands (Figure 1.24, L4–L10) in the hydrocyanation of styrene (Table 1.2) [90].

The extremes of this series behaved as expected; ligand L4 gave the poorest conversion and yield (16% and 12%, respectively) whilst the most electron-withdrawing ligand, L10, gave nearly total conversion (98%) and a yield of 90%. Moreover, a high degree of regioselectivity was maintained across the series (>99% in all cases).

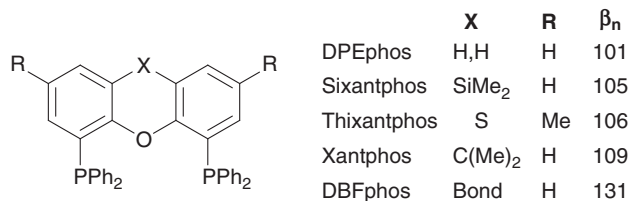


Figure 1.22 Series of wide bite angle diphosphine ligands.

Table 1.1 Nickel–phosphine catalysed hydrocyanation of styrene.

Ligand	β_n	Yield (%)	Branched product (%)
DPEphos	101	35–41	88–91
Sixantphos	105	94–95	97–98
Thixantphos	106	69–92	96–98
Xantphos	109	27–75	96–99
DBFphos	131	0.7	83
PPh ₃	—	0	—
DPPE	78	<1	ca. 40
DPPP	87	4–11	ca. 90
DPPB	98	3–8	92–95
BINAP	85	4	29

Source: Reproduced from [89].

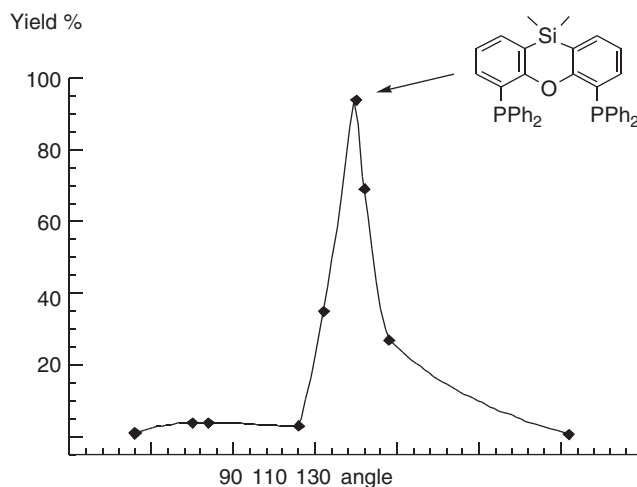


Figure 1.23 Effect of ligand bite angle on product yield in nickel-catalysed hydrocyanation of styrene.

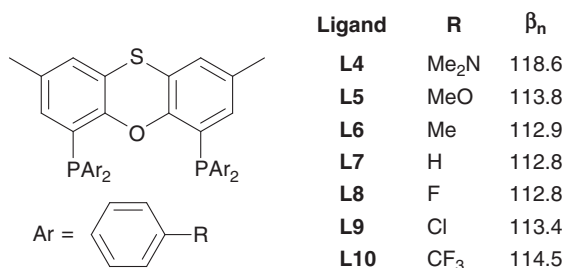


Figure 1.24 Electronically tuned Thixantphos ligands.

Table 1.2 Catalytic hydrocyanation of styrene.

Ligand	Conversion (%)	Yield (%)	Selectivity (%)	Regioselectivity (%)
L4	16	12	76	>99
L5	33	22	66	99.5
L6	55	48	87	99.8
L7	77	70	92	99.4
L8	46	38	83	99.4
L9	75	52	70	99.3
L10	98	90	92	99.0

Source: Reproduced from [90].

1.5 Conclusions

The development of organotransition metal chemistry has contributed significantly to the enormous growth of homogeneous catalysis. Knowledge about bonding and reactivity in organometallic chemistry has been of great support to catalysis. The reactivity of organotransition metal complexes is to an astounding extent dependent on the ligand environment around the metal. By changing the ligands, the catalysis can be

directed and sometimes the catalytic behaviour can even be predicted. Still, systematic studies involving small ligand families are the best way to elucidate detailed mechanistic information and investigate subtle ligand effects. The development of new and the optimisation of existing catalytic reactions can be achieved via the rational design of ligands. The development of qualitative and quantitative ligand parameters has proven to be an increasingly useful tool in this respect.

Computational methods have become increasingly important in catalyst development. Not only have advanced higher level theoretical methods contributed enormously to mechanistic understanding of catalytic reactions, but also proper development of ligand descriptors has contributed to the discovery of completely new families of ligands, catalysts derived from them and even new catalytic transformations. The rapid growth of knowledge and understanding of catalytic reactions in combination with advances in computational design will undoubtedly lead to further improvement of rational ligand design.

Arguably, phosphorus donor compounds are among the most successfully applied ligands in homogeneous catalysis. This might be due to the vast amount of detailed structural information that is readily available by, for example, *in situ* ^{31}P NMR. This has definitely contributed to proper understanding of ligand effects and the development of reliable ligand parameters. Computational approaches such as ligand knowledge bases have already led to the discovery of unexpected ligand structures that were less likely to be explored by experimental catalysis researchers. In this book, we decided to include not only ligands which have shown ample successful applications in homogeneous catalysis, such as phosphines and phosphites, but also ligand classes which have been considered as chemical curiosities for a long time. There are many phosphorus compounds out there which have been studied only by fundamental main group chemists and are considered to be difficult to prepare and handle. These compounds, however, might possess the right steric and electronic ligand properties required for novel catalysts to be discovered. To facilitate the introduction of less studied ligand groups in new areas, we have included representative experimental procedures provided by experts in the field for each class of ligands described in the following chapters.

References

- [1] R. Noyori, *Angew. Chem. Int. Ed.* **2002**, *41*, 2008.
- [2] W. S. Knowles, *Angew. Chem. Int. Ed.* **2002**, *41*, 1998.
- [3] R. H. Grubbs, *Angew. Chem. Int. Ed.* **2006**, *45*, 3760.
- [4] E.-i. Negishi, *Angew. Chem. Int. Ed.* **2011**, *50*, 6738.
- [5] A. Suzuki *Angew. Chem. Int. Ed.* **2011**, *50*, 6722.
- [6] W. S. Knowles, M. J. Sabacky, D. Vineyard, *J. Chem. Soc., Chem. Commun.* **1972**, 10.
- [7] W. S. Knowles, M. J. Sabacky, B. D. Vineyard, D. J. Weinkauff, *J. Am. Chem. Soc.* **1975**, *97*, 2567.
- [8] M. van den Berg, A. J. Minnaard, E. P. Schudde, J. van Esch, A. H. M. de Vries, J. G. de Vries, B. L. Feringa, *J. Am. Chem. Soc.* **2000**, *122*, 11539.
- [9] (a) J. E. Babin, G. T. Whiteker, W.O. 93 03839, US Pat. 911 518, **1992** (to Union Carbide Corporation); *Chem. Abstr.* **1993**, *119*, 159872; (b) G. J. H. Buisman, E. J. Vos, P. C. J. Kamer, P. W. N. M. van Leeuwen, *J. Chem. Soc. Dalton Trans.* **1995**, 409; and (c) G. J. H. Buisman, L. A. van der Veen, A. Klootwijk, W. G. J. de Lange, P. C. J. Kamer, P. W. N. M. van Leeuwen, D. Vogt, *Organometallics* **1997**, *16*, 2929.
- [10] N. Sakai, S. Mano, K. Nozaki, H. Takaya, *J. Am. Chem. Soc.* **1993**, *115*, 7033.
- [11] B. M. Trost, D. L. Van Vranken, *Angew. Chem. Int. Ed.* **1992**, *31*, 228.
- [12] A. Pfaltz, R. Prétôt, *Angew. Chem. Int. Ed.* **1998**, *37*, 323.
- [13] (a) P. Dierkes, S. Ramdeehul, L. Barloy, A. De Cian, J. Fischer, P. C. J. Kamer, P. W. N. M. van Leeuwen, J. A. Osborn, *Angew. Chem., Int. Ed.* **1998**, *37*, 3116; and (b) S. Ramdeehul, P. Dierkes, R. Aguado, P. C. J. Kamer, P. W. N. M. van Leeuwen, J. A. Osborn, *Angew. Chem. Int. Ed.* **1998**, *37*, 3118.
- [14] T. P. Yoon, E. N. Jacobsen, *Science* **2003**, *299*, 1691.
- [15] W. Reppe, W. J. Schweckendiek, *Annalen* **1948**, *104*, 560.

- [16] O. Roelen, Chemische Verwertungsgesellschaft Oberhausen m.b.H., **1938/1952**, DE 849548, Germany; O. Roelen, *Chem. Exp. Didakt.* **1977**, 3, 119; and O. Roelen, Chemische Verwertungsgesellschaft Oberhausen m.b.H., **1943**, US 2327066.
- [17] W. C. Drinkard, R. V. Lindsey, Du Pont, **1970**, US 3655723; E. S. Brown, In *Aspects of Homogeneous Catalysis*; R. Ugo, Ed., Reidel, **1974**, Vol. 2, 57–78.
- [18] C. A. Tolman, *Chem. Rev.* **1977**, 77, 313.
- [19] J. F. Young, J. A. Osborn, F. A. Jardine, G. Wilkinson *J. Chem. Soc., Chem. Comm.* **1965**, 131.
- [20] C. O'Connor, G. Wilkinson, *Tetrahedron Lett.* **1969**, 18, 1375.
- [21] L. Vaska, R. E. Rhodes, *J. Am. Chem. Soc.* **1965**, 87, 4970.
- [22] D. Evans, J. A. Osborn, G. Wilkinson, *J. Chem. Soc. A.* **1968**, 3133; and F. H. Jardine, J. A. Osborn, G. Wilkinson, J. F. Young, *Chem. and Ind. (London)* **1965**, 560.
- [23] R. L. Pruett, J. A. Smith, *J. Org. Chem.* **1969**, 34, 327.
- [24] K. Issleib, D. W. Müller, *Chem. Ber.* **1959**, 92, 3175.
- [25] W. Hieber, W. Freyer, *Chem. Ber.* **1960**, 93, 462; J. Chatt, W. J. Hart, *J. Chem. Soc.* **1960**, 1378.
- [26] L. G. Cannel, L. H. Slaugh, R. D., Mullineaux, Shell Development, **1960**, DE 1186455.
- [27] R. S. Bauer, P. W. Glockner, W. Keim, H. van Zwet, H. Chung, Shell Development, **1972**, US 3644563.
- [28] M. Iwamoto, S. Yuguchi, *J. Org. Chem.* **1966**, 31, 4290.
- [29] D. L. Thorn, R. J. Hoffmann, *Am. Chem. Soc.* **1978**, 100, 2079.
- [30] T. P. Dang, H. B. Kagan, *J. Am. Chem. Soc.* **1972**, 92, 6429.
- [31] J. C. Poulin, T. P. Dang, H. B. Kagan, *J. Organomet. Chem.* **1975**, 84, 87.
- [32] R. Selke, H. Pracejus, *J. Mol. Catal.* **1986**, 37, 213.
- [33] A. Miyashita, A. Yasuda, H. Tanaka, K. Toriumi, T. Ito, T. Souchi, R. Noyori, *J. Am. Chem. Soc.* **1980**, 102, 7932.
- [34] M. J. Burk, *J. Am. Chem. Soc.* **1991**, 113, 8518.
- [35] A. Togni, *Angew. Chem.* **1993**, 108, 1581.
- [36] *Metal-catalyzed Cross-coupling Reactions*, F. Diederich, P. J. Stang, Eds., Wiley-VCH, **1998**.
- [37] M-N. Birkholz (née Gensow), Z. Freixa, P. W. N. M. van Leeuwen, *Chem. Soc. Rev.*, **2009**, 38, 1099.
- [38] B. M. Trost, D. J. Murphy, *Organometallics* **1985**, 4, 1143.
- [39] C. P. Butts, E. Filali, G. C. Lloyd-Jones, P.-O. Norrby, D. A. Sale, Y. Schramm, *J. Am. Chem. Soc.* **2009**, 131, 9945.
- [40] M. Beller, T. H. Riermeijer, S. Haber, H. J. Kleiner, W. A. Herrmann, *Chem. Ber.* **1996**, 129, 1259.
- [41] D. A. Albiison, R. B. Bedford, S. E. Lawrence, P. N. Scully, *J. Chem. Soc., Chem. Commun.* **1998**, 2095.
- [42] G. P. F. van Strijdonck, M. D. K. Boele, P. C. J. Kamer, J. G. de Vries, P. W. N. M. van Leeuwen, *Eur. J. Inorg. Chem.* **1999**, 1073.
- [43] P. W. N. M. van Leeuwen, C. F., Roobeek, Shell Oil, GB 2068377 and US 4467116.
- [44] A. van Rooy, E. N. Orij, P. C. J. Kamer, P. W. N. M. van Leeuwen, *Organometallics* **1995**, 14, 34; T. Jongsma, B. Challa, P. W. N. M. van Leeuwen, *J. Organomet. Chem.* **1991**, 421, 121; and P. W. N. M. van Leeuwen, C. F. Roobeek, *J. Organomet. Chem.* **1983**, 258, 343.
- [45] L. H. Slaugh, R. D. Mullineaux, *J. Organomet. Chem.* **1968**, 13, 469; and J. L. Van Winkle, S. Lorenzo, R. C. Morris, R. F. Mason, US Patent, 3,420,898, **1969**, US Appl. 1965-443703, *Chem. Abstr.* **1967**, 66, 65101.
- [46] T. Onoda, *Chem. Tech.* **1993**, Sept., 34.
- [47] E. Billig, A. G. Abatjoglou, D. R. Bryant, R. E. Murray, J. M., Maher, Union Carbide Corp., **1986**, US 4599206.
- [48] E. Billig, A. G. Abatjoglou, D. R., Bryant, Union Carbide Corp., **1987**, US 4769498, US 4668651 and US 4748261.
- [49] N. Yoshinura, Y. Tokito, Kuraray, EP 223103.
- [50] C. P. Casey, G. T. Whiteker, M. G. Melville, L. M. Petrovich, J. A. Gavney Jr., D. R. Powell, *J. Am. Chem. Soc.* **1992**, 114, 5535.
- [51] C. P. Casey, G. T. Whiteker, *Isr. J. Chem.* **1990**, 20, 299.
- [52] M. Kranenburg, Y. E. M. van der Burgt, P. C. J. Kamer, P. W. N. M. van Leeuwen, K. Goubitz, J. Fraanje, *Organometallics* **1995**, 14, 3081.
- [53] P. C. J. Kamer, P. W. N. M. van Leeuwen, J. N. H. Reek, *Acc. Chem. Res.* **2001**, 34, 895.
- [54] W. Strohmeier, F. J. Müller, *Chem. Ber.* **1967**, 100, 2812.
- [55] C. A. Tolman, *J. Am. Chem. Soc.* **1970**, 92, 2953.
- [56] A. Roodt, S. Otto, G. Steyl, *Coord. Chem. Rev.* **2003**, 245, 121.

- [57] S. X. Xiao, W. C. Trogler, D. E. Ellis, Z. Berkovitch-Yellin, *J. Am. Chem. Soc.* **1983**, *105*, 7033; D. S. Marynick, *J. Am. Chem. Soc.* **1984**, *106*, 4064; J. A. Tossel, J. H. Moore, J. C. Giordan, *Inorg. Chem.* **1985**, *24*, 1100; and A. G. Orpen, N. G. Connelly, *Organometallics* **1990**, *9*, 1206.
- [58] R. S. Drago, S. Joerg, *J. Am. Chem. Soc.* **1996**, *118*, 2654.
- [59] S. Joerg, R. S. Drago, J. Sales, *Organometallics* **1998**, *17*, 589.
- [60] W. A. G. Graham, *Inorg. Chem.* **1968**, *7*, 315; and R. P. Stewart, P. M. Teichel, *Inorg. Chem.* **1968**, *7*, 1942.
- [61] M. N. Golovin, M. M. Rahman, J. E. Belmonte, W. P. Giering, *Organometallics* **1985**, *4*, 1981; and A. Fernandez, M. R. Wilson, D. C. Woska, A. Prock, W. P. Giering, C. M. Haar, S. P. Nolan, B. M. Foxman, *Organometallics* **2002**, *21*, 2758.
- [62] S. Tobisch, T. Ziegler, *J. Am. Chem. Soc.* **2002**, *124*, 13290.
- [63] D. Gleich, J. Hutter, *Chem. Eur. J.* **2004**, *10*, 2435.
- [64] G. Pacchioni, P. S. Bagus, *Inorg. Chem.* **1992**, *31*, 4391.
- [65] O. Gonzalez-Blanco, V. Branchadell, *Organometallics* **1997**, *16*, 5556.
- [66] C. R. Landis, S. Feldgus, J. Uddin, C. E. Wozniak, *Organometallics* **2000**, *19*, 4878.
- [67] T. L. Brown, K. J. Lee, *Coord. Chem. Rev.* **1993**, *128*, 89.
- [68] D. White, B. C. Tavener, N. J. Coville, P. W. Wade, *J. Organomet. Chem.* **1995**, *495*, 41.
- [69] T. L. Brown, *Inorg. Chem.* **1992**, *31*, 1286.
- [70] Y. Koide, S. G. Bott, A. R. Barron, *Organometallics*, **1996**, *15*, 2213.
- [71] K. Angermund, W. Baumann, E. Dinjus, R. Fornika, H. Goerls, M. Kessler, C. Krueger, W. Leitner, F. Lutz, *Chem.-Eur. J.*, **1997**, *3*, 755.
- [72] F. Maseras, K. Morokuma, *J. Comput. Chem.* **1995**, *16*, 1170; and M. Svensson, S. Humbel, R. D. J. Froese, T. Matsubara, S. Sieber, K. Morokuma, *J. Phys. Chem.* **1996**, *100*, 19357.
- [73] C. R. Landis, S. Feldgus, *Angew. Chem. Int. Ed.* **2000**, *39*, 2863; S. Feldgus, C. R. Landis, *J. Am. Chem. Soc.* **2000**, *122*, 12714.
- [74] S. Feldgus, C. R. Landis, *Organometallics* **2001**, *20*, 2374.
- [75] A. M. Segarra, E. Daura-Oller, C. Claver, J. M. Poblet, C. Bo, E. Fernandez, *Chem. Eur. J.* **2004**, *10*, 6456.
- [76] D. Gleich, R. Schmid, W. A. Herrmann, *Organometallics* **1998**, *17*, 4828; J. J. Carbo, F. Maseras, C. Bo, P. W. N. M. van Leeuwen, *J. Am. Chem. Soc.* **2001**, *123*, 7630; S. A. Decker, T. R. Cundari, *J. Organomet. Chem.* **2001**, *635*, 132; and C. R. Landis, J. Uddin, *J. Chem. Soc., Dalton Trans.* **2002**, 729.
- [77] A. Magistrato, A. Togni, U. Rothlisberger, *Organometallics* **2006**, *25*, 1151.
- [78] K. Vanka, Z. T. Xu, T. Ziegler, *Organometallics* **2005**, *23*, 419; and L. Q. Deng, T. K. Woo, L. Cavallo, P. M. Margl, T. Ziegler, *J. Am. Chem. Soc.* **1997**, *119*, 6177.
- [79] P. Dierkes, P. W. N. M. van Leeuwen, *J. Chem. Soc., Dalton Trans.* **1999**, 1519.
- [80] P. W. N. M. van Leeuwen, P. C. J. Kamer, J. N. H. Reek, P. Dierkes, *Chem. Rev.* **2000**, *100*, 2741.
- [81] Z. Freixa, P. W. N. M. van Leeuwen, *J. Chem. Soc., Dalton Trans.* **2003**, 1890.
- [82] S. Otsuka, *J. Organomet. Chem.* **1980**, *200*, 191.
- [83] A. Miedaner, R. C. Haltiwanger, D. L. DuBois, *Inorg. Chem.* **1991**, *30*, 417.
- [84] D. E. Berning, B. C. Noll, D. L. DuBois, *J. Am. Chem. Soc.* **1999**, *121*, 11432; and J. W. Raebiger, A. Miedaner, C. J. Curtis, S. M. Miller, O. P. Anderson, D. L. DuBois, *J. Am. Chem. Soc.* **2004**, *126*, 5502.
- [85] R. J. Angelici, *Acc. Chem. Res.* **1995**, *28*, 51.
- [86] R. J. van Haaren, H. Oevering, B. B. Coussens, G. P. F. van Strijdonck, J. N. H. Reek, P. C. J. Kamer, P. W. N. M. van Leeuwen, *Eur. J. Inorg. Chem.* **1999**, 1237.
- [87] B. M. Trost, D. L. van Vranken, C. Bingel, *J. Am. Chem. Soc.* **1992**, *114*, 9327.
- [88] W. J. van Zeist, R. Visser, F. M. Bickelhaupt, *Chem.-Eur. J.*, **2009**, *15*, 6112.
- [89] M. Kranenburg, P. C. J. Kamer, P. W. N. M. van Leeuwen, D. Vogt, W. Keim, *J. Chem. Soc., Chem. Commun.*, **1995**, 2177.
- [90] W. Goertz, W. Keim, D. Vogt, U. Englert, M. D. K. Boele, L. A. van der Veen, P. C. J. Kamer, P. W. N. M. van Leeuwen, *J. Chem. Soc., Dalton Trans.*, **1998**, 2981.
- [91] E. Zuidema, P. W. N. M. van Leeuwen, C. Bo, *Organometallics*, **2005**, *15*, 3703.
- [92] O. Kühn, *Coord. Chem. Rev.* **2005**, *249*, 693.
- [93] C. H. Suresh, N. Koga, *Inorg. Chem.* **2002**, *41*, 1573.

- [94] C. H. Suresh, *Inorg. Chem.* **2006**, *45*, 4982.
- [95] N. Fey, A. G. Orpen, J. N. Harvey, *Coord. Chem. Rev.* **2009**, *253*, 704.
- [96] N. Fey, J. N. Harvey, G. C. Lloyd-Jones, P. Murray, A. G. Orpen, R. Osborne, M. Purdie, *Organometallics* **2008**, *27*, 1372.
- [97] P. G. Pringle, *Angew. Chem. Int. Ed.* **submitted**.
- [98] E. Burello, G. Rothenberg, *Int. J. Mol. Sci.* **2006**, *7*, 375.
- [99] E. Burello, P. Marion, J. C. Galland, A. Chamard, G. Rothenberg, *Adv. Synth. Catal.* **2005**, *347*, 803.
- [100] E. Burello, G. Rothenberg, *Adv. Synth. Catal.* **2005**, *347*, 1969.
- [101] J. A. Hageman, J. A. Westerhuis, H. W. Fruhauf, G. Rothenberg, *Adv. Synth. Catal.* **2006**, *348*, 361.
- [102] A. G. Maldonado, J. A. Hageman, S. Mastroianni, G. Rothenberg, *Adv. Synth. Catal.* **2009**, *351*, 387.
- [103] W. S. Knowles, M. J. Sabacky, *Chem. Commun.* **1968**, 1445.
- [104] M. D. Fryzuk, B. Bosnich, *J. Am. Chem. Soc.* **1979**, *101*, 3043; and T. P. Dang, H. B. Kagan, *J. Chem. Soc. Chem. Commun.* **1971**, 481.
- [105] W. S. Knowles, *Acc. Chem. Res.* **1983**, *16*, 106; and B. D. Vineyard, W. S. Knowles, M. J. Sabacky, G. L. Bachman, D. J. Weinkauff, *J. Am. Chem. Soc.* **1977**, *99*, 5946.
- [106] C. R. Landis, J. Halpern, *J. Am. Chem. Soc.* **1987**, *109*, 1746; J. Halpern, *Science* **1982**, *217*, 401; and A. S. C. Chan, J. J. Pluth, J. Halpern, *J. Am. Chem. Soc.* **1980**, *102*, 5952.
- [107] J. M. Brown, P. A. Chaloner, *J. Am. Chem. Soc.* **1980**, *102*, 3040.
- [108] R. Noyori, H. Takaya, *Acc. Chem. Res.* **1990**, *23*, 345; T. Imamoto, J. Watanabe, Y. Wada, H. Masuda, H. Yamada, H. Tsuruta, S. Matsukawa, K. Yamaguchi, *J. Am. Chem. Soc.* **1998**, *120*, 1635; E. Fernandez, A. Gillon, K. Heslop, E. Horwood, D. J. Hyett, A. G. Orpen, P. G. Pringle, *Chem. Commun.* **2000**, 1663; M. J. Burk, J. E. Feaster, W. A. Nugent, R. L. Harlow, *J. Am. Chem. Soc.* **1993**, *115*, 10125; and M. J. Burk, *Accounts Chem. Res.* **2000**, *33*, 363.
- [109] K. Matsumura, H. Shimizu, T. Saito, H. Kumobayashi, *Adv. Synth. Catal.* **2003**, *345*, 180; G. Hoge, H. P. Wu, W. S. Kissel, D. A. Pflum, D. J. Greene, J. Bao, *J. Am. Chem. Soc.* **2004**, *126*, 5966; and S. Basra, J. G. de Vries, D. J. Hyett, G. Harrison, K. M. Heslop, A. G. Orpen, P. G. Pringle, K. von der Luehe, *Dalton Trans.* **2004**, 1901.
- [110] A. Togni, C. Breutel, A. Schnyder, F. Spindler, H. Landert, A. Tijani, *J. Am. Chem. Soc.* **1994**, *116*, 4062; T. V. RajanBabu, A. L. Casalnuovo, *J. Am. Chem. Soc.* **1996**, *118*, 6325; K. W. Kottsieper, U. Kuhner, O. Stelzer, *Tetrahedron: Asymmetry* **2001**, *12*, 1159; P. Kocovsky, S. Vyskocil, M. Smrcina, *Chem. Rev.* **2003**, *103*, 3213; T. Hayashi, M. Kumada, *Acc. Chem. Res.* **1982**, *15*, 395; S. Castillon, C. Claver, Y. Diaz, *Chem. Soc. Rev.* **2005**, *34*, 702; and K. Achiwa, *J. Am. Chem. Soc.* **1976**, *98*, 8265.
- [111] H. Zabrodsky, D. Avnir, *J. Am. Chem. Soc.* **1995**, *117*, 462.
- [112] K. B. Lipkowitz, S. Schefzick, D. Avnir, *J. Am. Chem. Soc.* **2001**, *123*, 6710; and J. W. Handgraaf, J. N. H. Reek, L. Bellarosa, F. Zerbetto, *Adv. Synth. Catal.* **2005**, *347*, 792.
- [113] D. Q. Gao, S. Schefzick, K. B. Lipkowitz, *J. Am. Chem. Soc.* **1999**, *121*, 9481.
- [114] K. B. Lipkowitz, T. Sakamoto, J. Stack, *Chirality* **2003**, *15*, 759; and K. B. Lipkowitz, C. A. D'Hue, T. Sakamoto, J. N. Stack, *J. Am. Chem. Soc.* **2002**, *124*, 14255.
- [115] J. E. Backvall, O. S. Andell, *J. Chem. Soc., Chem. Commun.*, **1981**, 1098–1099.
- [116] W. R. Jackson, C. G. Lovel, *Tetrahedron Lett.*, **1982**, *23*, 1621–1624.
- [117] J. E. Backvall, O. S. Andell, *J. Chem. Soc., Chem. Commun.*, **1984**, 260–261.
- [118] C. A. Tolman, W. C. Seidel, J. D. Druliner, P. J. Dommille, *Organometallics*, **1984**, *3*, 33–38.
- [119] J. D. Druliner, *Organometallics*, **1984**, *3*, 205–208.
- [120] R. J. McKinney, D. C. Roe, *J. Am. Chem. Soc.*, **1985**, *107*, 261–262.
- [121] J. E. Backvall, O. S. Andell, *Organometallics*, **1986**, *5*, 2350–2355.
- [122] R. J. McKinney, D. C. Roe, *J. Am. Chem. Soc.*, **1986**, *108*, 5167–5173.
- [123] J. Wiltling, C. Muller, A. C. Hewat, D. D. Ellis, D. M. Tooke, A. L. Spek, D. Vogt, *Organometallics*, **2005**, *24*, 13–15.
- [124] M. J. Baker, P. G. Pringle, *J. Chem. Soc., Chem. Commun.*, **1991**, 1292–1293.
- [125] M. J. Baker, K. N. Harrison, A. G. Orpen, P. G. Pringle, G. Shaw, *J. Chem. Soc., Chem. Commun.*, **1991**, 803–804.